

# Fluorometric Chemosensors. Interaction of Toxic Heavy Metal Ions Pb<sup>II</sup>, Cd<sup>II</sup>, and Hg<sup>II</sup> with Novel Mixed-Donor Phenanthroline-Containing Macrocycles: Spectrofluorometric, Conductometric, and Crystallographic Studies

M. Carla Aragoni,<sup>†</sup> Massimiliano Arca,<sup>†</sup> Francesco Demartin,<sup>†</sup> Francesco A. Devillanova,<sup>†</sup> Francesco Isaia,<sup>†</sup> Alessandra Garau,<sup>†</sup> Vito Lippolis,<sup>\*,†</sup> Fahimeh Jalali,<sup>§</sup> Ulrich Papke,<sup>||</sup> Mojtaba Shamsipur,<sup>§</sup> Lorenzo Tei,<sup>†</sup> Abdollah Yari,<sup>§</sup> and Gaetano Verani<sup>†</sup>

Dipartimento di Chimica Inorganica ed Analitica, Università degli Studi di Cagliari, SS 554 Bivio per Sestu, 09042 Monserrato (CA), Italy, Dipartimento di Chimica Strutturale e Stereochimica Inorganica, Università di Milano, Via G. Venezian 21, 20133 Milano, Italy, Department of Chemistry, Razi University, Kermanshah, Iran, and Institut für Organische Chemie der Technischen Universität, Braunschweig, Hagenring 30, D 38106 Braunschweig, Germany

Received April 12, 2002

The macrocycles L<sup>1</sup>–L<sup>3</sup> incorporating N<sub>2</sub>S<sub>3</sub><sup>-</sup>, N<sub>2</sub>S<sub>2</sub>O<sup>-</sup>, and N<sub>2</sub>S<sub>2</sub>-donor sets, respectively, and containing the 1,10-phenanthroline unit interact in acetonitrile solution with heavy metal ions such as Pb<sup>II</sup>, Cd<sup>II</sup>, and Hg<sup>II</sup> to give 1:1 ML, 1:2 ML<sub>2</sub>, and 2:1 M<sub>2</sub>L complex species, which specifically modulate the photochemical properties of the ligands. The stoichiometry of the complex species formed during spectrofluorometric titrations and their formation constants in MeCN at 25 °C were determined from fluorescence vs M<sup>II</sup>/L molar ratio data. The complexes [Pb(L<sup>1</sup>)](ClO<sub>4</sub>)<sub>2</sub>·½H<sub>2</sub>O (**1**), [Pb(L<sup>2</sup>)](ClO<sub>4</sub>)<sub>2</sub>·MeNO<sub>2</sub> (**1a**), [Pb(L<sup>3</sup>)<sub>2</sub>](ClO<sub>4</sub>)<sub>2</sub>·2MeCN (**1b**), and [Cd(L<sup>3</sup>)](NO<sub>3</sub>)<sub>2</sub> (**2b**) were also characterized by X-ray diffraction studies. The conformation adopted by L<sup>1</sup>–L<sup>3</sup> in these species reveals the aliphatic portion of the rings folded over the plane containing the heteroaromatic moiety with the ligands trying to encapsulate the metal center within their cavity. In **1**, **1a**, and **2b** the metal ion completes the coordination sphere by interacting with counteranion units and solvent molecules. On the contrary, the 1:2 complex **1b** shows Pb<sup>II</sup> sandwiched between two symmetry-related molecules of L<sup>3</sup> reaching an overall [4N + 4S] eight-coordination.

## Introduction

The sustained interest in the coordination chemistry of lead(II), cadmium(II), and mercury(II) stems not only from the widespread agricultural and industrial use of their compounds but also from their inherent toxicity and hazardous effects to human health.<sup>1,2</sup> In this respect, of crucial importance is the design and development of efficient complexing agents that may be used as selective extractants

of these environmentally important metal ions and as sensors for their detection in solution.<sup>3–7</sup> With regard to molecular recognition and selective binding, macrocyclic ligands are extensively studied.<sup>5–8</sup> In fact, by changing some structural features of the macrocyclic framework such as number and

\* To whom correspondence should be addressed. Phone: +30 0706754467.

Fax: +30 0706754456. E-mail: lippolis@unica.it.

<sup>†</sup> Università degli Studi di Cagliari.

<sup>‡</sup> Università di Milano.

<sup>§</sup> Razi University.

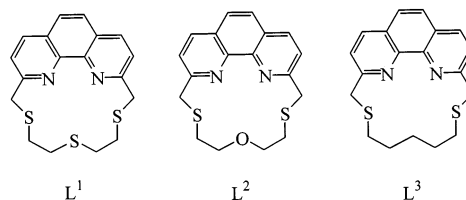
<sup>||</sup> Technischen Universität Braunschweig.

- (1) Kaim, W.; Schwederski, B. *Bioinorganic Chemistry: Inorganic Elements in the Chemistry of Life, an Introduction and Guide*; Wiley-Interscience: New York, 1991.
- (2) Klassen, C. D.; Amdur, M. D.; Dull, J. *Casarett and Doull's Toxicology*, 3rd ed.; MacMillan: New York, 1986.

- (3) (a) *Macrocyclic Compounds in Analytical Chemistry*; Zolotov, Yu. A., Ed.; Wiley: New York, 1997. (b) Yordanov, A. T.; Roundhill, D. M. *Coord. Chem. Rev.* **1998**, *170*, 93.
- (4) (a) Yamini, Y.; Alizadeh, N.; Shamsipur, M. *Anal. Chim. Acta* **1997**, *355*, 69. (b) Kodama, M.; Kimura, E. *Bull. Chem. Soc. Jpn.* **1989**, *62*, 3093.
- (5) (a) Bazzicalupi, C.; Bencini, A.; Fusi, V.; Giorgi, C.; Paoletti, P.; Valtancoli, B. *J. Chem. Soc., Dalton Trans.* **1999**, 393 and references therein. (b) Esteban, D.; Bañobre, D.; de Blas, A.; Rodríguez-Blas, T.; Bastida, R.; Macías, A.; Rodríguez, A.; Fenton, D. E.; Adams, H.; Mahía, J. *Eur. J. Inorg. Chem.* **2000**, 1445.
- (6) (a) Adam, K. R.; Baldwin, D. S.; Duckworth, P. A.; Lindoy, L. F.; McPartlin, M.; Bashall, A.; Powell, H. R.; Tasker, P. A. *J. Chem. Soc., Dalton Trans.* **1995**, 1127. (b) Ahearn, M.-A.; Kim, J.; Leong, A. J.; Lindoy, L. F.; Matthews, O. A.; Meehan, G. V. *J. Chem. Soc., Dalton Trans.* **1996**, 3591.

disposition of donor atoms, cavity size, and conformational flexibility, it is possible to design highly preorganized ligands capable of recognizing and binding selectively to certain metal ion guests. On the other hand, one of the most attractive and sensitive methods for signaling the host–guest recognition event is based on the use of fluorescent receptors, which undergo a specific emission spectral change upon selective binding to the guest.<sup>9</sup> Many selective sensors and switches of fluorescence have been synthesized in the past few years which comprise fluorophores such as anthracene,<sup>10a–d</sup> 8-hydroxyquinoline,<sup>10e</sup> dansylamide,<sup>9b</sup> or phenanthroline<sup>11,12</sup> as a signaling site, either connected to a macrocyclic unit as sidearms or inserted as nonpendant integral part of a macrocyclic structure. Recently, we reported the synthesis and coordination properties toward some platinum-group transition metal ions (Ni<sup>II</sup>, Pd<sup>II</sup>, Pt<sup>II</sup>, Rh<sup>III</sup>, Ru<sup>II</sup>) of the mixed-donor crowns L<sup>1</sup> and L<sup>2</sup> containing the 1,10-phenanthroline unit as an integral part of the macrocyclic structure.<sup>13</sup> These macrocycles, analogously to those reported by Bencini et al.<sup>5a,12</sup> which contain polyamine chains linking the 2,9-phenanthroline positions, can be considered *intrinsic* fluorescent chemosensors with the thioether linkers functioning exclusively as binding sites and the phenanthroline unit playing both a signaling and a binding role. The presence in

L<sup>1</sup> and L<sup>2</sup> of thioether donors makes these ligands particularly attractive as potential fluorescent chemosensors for soft metal centers, in particular second and third row transition metal ions and post-transition heavy metals. The main aim of this paper was to investigate the coordination chemistry of the macrocycles L<sup>1</sup>, L<sup>2</sup>, and the new L<sup>3</sup> toward the toxic Pb<sup>II</sup>, Cd<sup>II</sup>, and Hg<sup>II</sup> metal ions to test the potentiality of these phenanthroline derivatives as specific fluorophores for the mentioned metal ions.



## Experimental Section

All melting points are uncorrected. Microanalytical data were obtained by using a Fisons EA CHNS-O instrument ( $T = 1000$  °C). EI mass spectra were obtained on a Fisons QMD 1000 mass spectrometer (70 eV, 200 mA, ion-source temperature 200 °C). FAB mass spectra were recorded at the Institut für Organische Chemie der Technischen Universität, Braunschweig. <sup>13</sup>C and <sup>1</sup>H NMR spectra were recorded on a Varian VXR300 spectrometer (operating at 75.4 MHz). The spectrophotometric measurements were carried out at 25 °C using a Varian model Cary 5 UV–vis–NIR spectrophotometer. All fluorescence spectra were recorded on a Perkin-Elmer LS-30 luminescence spectrometer, equipped with a xenon lamp. Conductance measurements were carried out with a Metrohm 712 conductivity meter. A dip-type conductivity cell made of platinum black was used. In all measurements, the cell was thermostated at  $25.0 \pm 0.1$  °C using a MLW thermostat.

The analytical grade nitrate salts of lead, cadmium, and mercury (all from Merck) used in the solution studies were of the highest purity available and were used without any further purification except for vacuum-drying over P<sub>2</sub>O<sub>5</sub>. Reagent grade acetonitrile (Merck) was used as received. Reagent perchlorate salts of lead and mercury for the complex synthesis were purchased by Aldrich and used without any further purification.

**Caution!** The Pb<sup>II</sup> and Hg<sup>II</sup> complexes of L<sup>1</sup>–L<sup>3</sup> were isolated in the solid state as ClO<sub>4</sub><sup>−</sup> salts. We worked with these complexes on a small scale without any incident. Despite these observations, the unpredictable behavior of ClO<sub>4</sub><sup>−</sup> salts necessitates extreme care in handling.

The dmf was dried with MgSO<sub>4</sub> and freshly distilled under vacuum. 2,9-Dimethyl-1,10-phenanthroline and 1,5-pentamethylene disulfide were commercially available.

L<sup>1</sup> and L<sup>2</sup> were synthesized and purified as described elsewhere.<sup>13</sup> L<sup>3</sup> was prepared by following a similar procedure.

**Synthesis of 2,8-Dithia[9](2,9)-1,10-phenanthrolinephane (L<sup>3</sup>).** A solution of 2,9-bis(chloromethyl)-1,10-phenanthroline<sup>13</sup> (0.5 g, 1.80 mmol) and 1,5-pentamethylene disulfide (0.25 g, 1.80 mmol) in dmf (40 cm<sup>3</sup>) was added, over 15 h, to a well-stirred suspension of Cs<sub>2</sub>CO<sub>3</sub> (1.18 g, 3.61 mmol) in dmf (80 cm<sup>3</sup>) maintained at 55 °C under N<sub>2</sub>. The resulting mixture was stirred for 1 h at 55 °C and for 24 h at room temperature and subsequently concentrated under reduced pressure. The obtained deep-yellow residue was purified by flash chromatography on silica gel using a mixture of CH<sub>2</sub>Cl<sub>2</sub>–MeCO<sub>2</sub>Et–EtOH (5:1:0.25 v/v/v ratio) as eluent to give 0.27 g (43.7% yield) of L<sup>3</sup> as a pale white product, mp 185 °C.

- (7) (a) Alcock, N. W.; Curzon, E. H.; Moore, P. J. *Chem. Soc., Dalton Trans.* **1984**, 2813. (b) Bashall, A.; McPartlin, M.; Murphy, B. P.; Powell, H. R.; Waikar, S. J. *Chem. Soc., Dalton Trans.* **1994**, 1383. (c) Luckay, R. C.; Hancock, R. D. J. *Chem. Soc., Dalton Trans.* **1991**, 1491.
- (8) (a) Bradshaw, J. S. *Aza-crown Macrocycles*; Wiley: New York, 1993. (b) Lindoy, L. F. *The Chemistry of Macrocyclic Ligand Complexes*; Cambridge University Press: Cambridge, U.K., 1989. (c) Döbler, M. *Ionophores and their Structure*; Wiley-Interscience: New York, 1981. (d) Hancock, R. D.; Martell, A. E. *Chem. Rev.* **1989**, 89, 1875. (e) Bradshaw, J. S.; Izatt, R. M. *Acc. Chem. Res.* **1997**, 30, 338.
- (9) (a) de Silva, A. P.; Nimal Gunaratne, H. Q.; Gunnlaugsson, T.; Huxley, A. J. M.; McCoy, C. P.; Rademacher, J. T.; Rice, T. E. *Chem. Rev.* **1997**, 97, 1515. (b) Kimura, E.; Koike, T. *Chem. Soc. Rev.* **1998**, 27, 179. (c) Fabbri, L.; Lichelli, M.; Parodi, L.; Poggi, A.; Taglietti, A. *Eur. J. Inorg. Chem.* **1999**, 35.
- (10) (a) Prodi, L.; Bolletta, F.; Montaldi, M.; Zaccaroni, N. *Coord. Chem. Rev.* **2000**, 205, 59. (b) Fabbri, L.; Lichelli, M.; Rabaioli, G.; Taglietti, A. *Coord. Chem. Rev.* **2000**, 205, 85. (c) Valeur, B.; Leray, I. *Coord. Chem. Rev.* **2000**, 205, 3. (d) Ciampolini, M.; Formica, M.; Fusi, V.; Saint-Maurice, A.; Micheloni, M.; Nardi, N.; Pontellini, R.; Pina, F.; Romani, P.; Sabatini, A. M.; Valtancoli, B. *Eur. J. Inorg. Chem.* **1999**, 2261. (e) Prodi, L.; Bargossi, C.; Montalti, M.; Zaccaroni, N.; Su, N.; Bradshaw, J. S.; Izatt, R. M.; Sauvage, P. B. J. *Am. Chem. Soc.* **2000**, 122, 6769.
- (11) (a) Sugihara, H.; Hiratami, K. *Coord. Chem. Rev.* **1996**, 148, 285. (b) Armaroli, N.; De Cola, L.; Balzani, V.; Sauvage, J.-P.; Dietrich-Buchecker, C. O.; Kern, J.-M.; Bailal, A. J. *Chem. Soc., Dalton Trans.* **1993**, 3241. (c) Kern, J.-M.; Sauvage, J.-P.; Weidmann, J.-L.; Armaroli, N.; Flamigni, L.; Ceroni, P.; Balzani, V. *Inorg. Chem.* **1997**, 36, 5329.
- (12) (a) Bazzicalupi, C.; Bencini, A.; Bianchi, A.; Giorgi, C.; Fusi, V.; Valtancoli, B.; Bernardo, M. A.; Pina, F. *Inorg. Chem.* **1999**, 38, 3806. (b) Bencini, A.; Bernardo, M. A.; Bianchi, A.; Fusi, V.; Giorgi, C.; Pina, F.; Valtancoli, B. *Eur. J. Inorg. Chem.* **1999**, 1911. (c) Bencini, A.; Bianchi, A.; Lodeiro, C.; Masotti, A.; Parola, A. J.; Pina, F.; Seixas de Melo, J.; Valtancoli, B. *Chem. Commun.* **2000**, 1639.
- (13) (a) Blake, A. J.; Demartin, F.; Devillanova, F. A.; Garau, A.; Isaia, F.; Lippolis, V.; Schröder, M.; Verani, G. J. *Chem. Soc., Dalton Trans.* **1996**, 3705. (b) Contu, F.; Demartin, F.; Devillanova, F. A.; Garau, A.; Isaia, F.; Lippolis, V.; Salis, A.; Verani, G. J. *Chem. Soc., Dalton Trans.* **1997**, 4401. (c) Blake, A. J.; Casabò, J.; Devillanova, F. A.; Escriche, L.; Garau, A.; Isaia, F.; Lippolis, V.; Kivekas, R.; Muns, V.; Schröder, M.; Sillanpää, R.; Verani, G. J. *Chem. Soc., Dalton Trans.* **1999**, 1085. (d) Arca, M.; Blake, A. J.; Casabò, J.; Demartin, F.; Devillanova, F. A.; Garau, A.; Isaia, F.; Lippolis, V.; Kivekas, R.; Muns, V.; Schröder, M.; Verani, G. J. *Chem. Soc., Dalton Trans.* **2001**, 1180.

Anal. Found (calcd for  $C_{19}H_{20}N_2S_2$ ): C, 66.7 (67.0); H, 5.7 (5.9); N, 8.0 (8.2); S, 18.5 (18.8). NMR:  $^1H$  ( $CDCl_3$ ),  $\delta_H$  8.15 (d, 2H,  $J = 8.7$ ), 7.70 (s, 2H), 7.53 (d, 2H,  $J = 8.1$  Hz), 4.11 (s, 4H), 2.65 (m, 4H), 1.95 (m, 4H), 1.35 (m, 2H);  $^{13}C$  ( $CDCl_3$ ),  $\delta_C$  159.9, 145.0, 136.9, 127.2, 125.5, 122.7, 36.6, 30.7, 28.9, 28.4. Mass spectrum (electronic impact, EI):  $m/z$  340 ( $L^3$ ), 178 (Phen) with the correct isotopic distribution. Electronic spectrum ( $CH_2Cl_2$ ):  $\lambda = 235$  ( $\epsilon = 44\ 800$ ), 272 (21 300), 288 (19 100), 306 nm (10 060  $dm^3 \cdot mol^{-1} \cdot cm^{-1}$ ).

**Synthesis of  $[Pb(L^1)][ClO_4]_2 \cdot 1/2H_2O$  (1),  $[Pb(L^2)][ClO_4]_2 \cdot MeNO_2$  (1a), and  $[Pb(L^3)_2][ClO_4]_2 \cdot 2MeCN$  (1b).** A mixture of the appropriate ligand (20 mg) and  $Pb(ClO_4)_2 \cdot 3H_2O$  (1:1 molar ratio) in MeOH (20  $cm^3$ ) was refluxed under  $N_2$  for 1 h. **1**: Slow evaporation at room temperature of the reaction mixture gave well-shaped white crystals of  $[Pb(L^1)][ClO_4]_2 \cdot 1/2H_2O$  (48% yield). Mp: 220 °C (dec). Anal. Found (calcd for  $C_{18}H_{19}Cl_2N_2O_{8.5}PbS_3$ ): C, 27.7 (27.9); H, 2.6 (2.5); N, 3.6 (3.6); S, 12.4 (12.4). **1a**: Slow evaporation at room temperature of the reaction mixture gave a yellow solid which was recrystallized from MeNO<sub>2</sub> by slow diffusion of Et<sub>2</sub>O. Well-shaped white crystals of  $[Pb(L^2)][ClO_4]_2 \cdot MeNO_2$  were obtained (66% yield). Mp: 220 °C (dec). Anal. Found (calcd for  $C_{19}H_{21}Cl_2N_3O_{11}PbS_2$ ): C, 28.4 (28.2); H, 2.2 (2.6); N, 5.6 (5.2); S, 8.1 (7.9). **1b**: The reaction mixture was concentrated under vacuum, and the resulting white product was recrystallized from MeCN–MeNO<sub>2</sub> by Et<sub>2</sub>O diffusion to give well-shaped white crystals of  $[Pb(L^3)_2][ClO_4]_2 \cdot 2MeCN$  (53% yield). Mp: 235 °C (dec). Anal. Found (calcd for  $C_{42}H_{46}Cl_2N_6O_8PbS_4$ ): C, 43.2 (43.1); H, 3.7 (4.0); N, 6.8 (7.2); S, 10.9 (11.0). Fab mass spectrum for **1**:  $m/z$  665, 565; calcd for  $[^{207}Pb(L^1)ClO_4]^+$  and  $[^{207}Pb(L^1)]^+$ ,  $m/z$  665 and 566, respectively. Fab mass spectrum for **1a**:  $m/z$  649, 549; calcd for  $[^{207}Pb(L^2)ClO_4]^+$  and  $[^{207}Pb(L^2)]^+$ ,  $m/z$  648 and 549, respectively. Fab mass spectrum for **1b**:  $m/z$  647, 547; calcd for  $[^{207}Pb(L^3)ClO_4]^+$  and  $[^{207}Pb(L^3)]^+$ ,  $m/z$  647 and 548, respectively.

**Synthesis of  $[Cd(L^1)][NO_3]_2$  (2),  $[Cd(L^2)][NO_3]_2$  (2a), and  $[Cd(L^3)][NO_3]_2$  (2b).** A mixture of the appropriate ligand (20 mg) and  $Cd(NO_3)_2 \cdot 4H_2O$  (1:1 molar ratio) in MeOH (20  $cm^3$ ) was refluxed under  $N_2$  for 1 h. On cooling, a white microcrystalline solid formed having formulation  $[Cd(L)][NO_3]_2$  (yield (%): 48 (**2**); 64 (**2a**); 51 (**2b**)). Crystals of good quality were obtained only for **2b** by slow diffusion of Et<sub>2</sub>O in a MeCN solution of the microcrystalline product. Mp (°C): 240 (**2**), 260 (**2a**), 235 (**2b**) (with decomposition). Anal. Found (calcd for  $C_{18}H_{18}CdN_4O_6S_3$ , **2**): C, 36.3 (36.3); H, 3.1 (3.0); N, 9.2 (9.4); S, 15.7 (16.2). Found (calcd for  $C_{18}H_{18}CdN_4O_7S_2$ , **2a**): C, 37.4 (37.4); H, 2.9 (3.1); N, 9.5 (9.7); S, 11.2 (11.1). Found (calcd for  $C_{19}H_{20}CdN_4O_6S_2$ , **2b**): C, 39.5 (39.6); H, 3.5 (3.5); N, 9.6 (9.7); S, 10.7 (11.1). Fab mass spectrum for **2**:  $m/z$  534, 471; calcd for  $[^{112}Cd(L^1)NO_3]^+$  and  $[^{112}Cd(L^1)]^+$ ,  $m/z$  533 and 471, respectively. Fab mass spectrum for **2a**:  $m/z$  518, 455; calcd for  $[^{112}Cd(L^2)NO_3]^+$  and  $[^{112}Cd(L^2)]^+$ , 517 and 455, respectively. Fab mass spectrum for **2b**:  $m/z$  516, 453; calcd for  $[^{112}Cd(L^3)NO_3]^+$  and  $[^{112}Cd(L^3)]^+$ , 515 and 453, respectively.

**Synthesis of  $[Hg(L^1)][ClO_4]_2$  (3),  $[Hg(L^2)][ClO_4]_2$  (3a), and  $[Hg(L^3)][ClO_4]_2$  (3b).** A mixture of the appropriate ligand (20 mg) and  $Hg(ClO_4)_2 \cdot 3H_2O$  (1:1 molar ratio) in MeOH (30  $cm^3$ ) was refluxed under  $N_2$  for 5 h. The white product obtained had the  $[Hg(L)][ClO_4]_2$  formulation (yield (%): 32 (**3**); 54 (**3a**); 47 (**3b**)). Crystals of good quality were not obtained upon recrystallization. Mp (°C): 240 (**3**), 245 (**3a**), 245 (**3b**) (with decomposition). Anal. Found (calcd for  $C_{18}H_{18}Cl_2HgN_2O_8S_3$ , **3**): C, 28.4 (28.5); H, 2.0 (2.4); N, 3.2 (3.7); S, 12.4 (12.7). Found (calcd for  $C_{18}H_{18}Cl_2HgN_2O_9S_2$ , **3a**): C, 29.4 (29.1); H, 2.3 (2.4); N, 3.8 (3.8); S, 8.5 (8.6). Found (calcd for  $C_{19}H_{20}Cl_2HgN_2O_8S_2$ , **3b**): C, 30.6 (30.8); H, 2.8 (2.7); N, 4.3 (3.8); S, 8.5 (8.7). Fab mass spectrum for **3**:

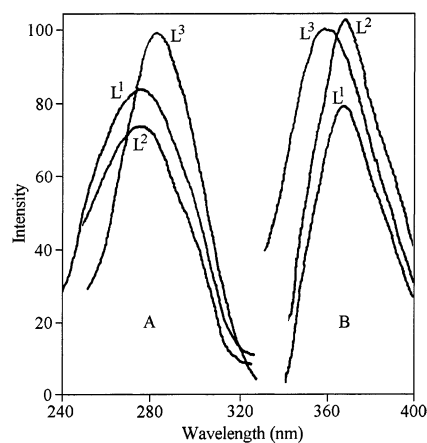


**Figure 1.** Excitation (A) and emission (B) spectra for  $1.0 \times 10^{-5}$  M solutions of the ligands  $L^1$ – $L^3$  in acetonitrile at 25 °C:  $\lambda_{ex} = 275$  nm for  $L^1$  and  $L^2$ , 285 nm for  $L^3$ ;  $\lambda_{em} = 365$  nm for  $L^1$  and  $L^2$ , 355 nm for  $L^3$ .

$m/z$  658, 558; calcd for  $[^{201}Hg(L^1)ClO_4]^+$  and  $[^{201}Hg(L^1)]^+$ , 658 and 559, respectively. Fab mass spectrum for **3a**:  $m/z$  643, 542; calcd for  $[^{201}Hg(L^2)ClO_4]^+$  and  $[^{201}Hg(L^2)]^+$ , 642 and 543, respectively. Fab mass spectrum for **3b**:  $m/z$  641, 540; calcd for  $[^{201}Hg(L^3)ClO_4]^+$  and  $[^{201}Hg(L^3)]^+$ , 641 and 540, respectively.

On using a 1:2  $M^{II}/L$  ( $M^{II} = Pb^{II}, Cd^{II}, Hg^{II}$ ;  $L = L^1$ – $L^3$ ) reaction molar ratio, the compounds reported above were always isolated.

**Spectrofluorometric Titrations and Calculations.** The experimental procedure for the spectrofluorometric titrations was as follow: A standard stock  $1.0 \times 10^{-3}$  M solution of each ligand was prepared by dissolving an appropriate amount of the ligand in a 50.0 mL precalibrated volumetric flask and diluting to the mark with MeCN. The titration solutions ( $1.0 \times 10^{-5}$  M) were prepared by appropriate dilution of the stock solution. Titration of the ligand solutions was then carried out by addition of microliter amounts of a concentrated standard solution of the metal ion of interest in MeCN using a precalibrated micropipet, followed by fluorescence intensity reading at 25 °C (14–23 data points) at the corresponding  $\lambda_{ex}$  and  $\lambda_{em}$ :  $\lambda_{ex} = 275$  nm for  $L^1$  and  $L^2$ , 285 nm for  $L^3$ ;  $\lambda_{em} = 365$  nm for  $L^1$  and  $L^2$ , 355 nm for  $L^3$  (see Figure 1). The stock solution of each cation ( $6.0 \times 10^{-4}$ – $5.0 \times 10^{-3}$  M) was prepared by direct exact weighing (with an accuracy of 0.000 01 g) of the pure nitrate salt vacuum-dried over  $P_2O_5$  in a precalibrated 50 mL volumetric flask and dilution to the mark with the solvent.

When a ligand, L, reacts with a metal ion,  $M^{2+}$ , it may form a 1:1  $ML$  (model I), both 1:1 and 1:2  $ML_2$  (model II), or both 1:1 and 2:1  $M_2L$  complexes (model III). The mass balances of the three possible models in solution can be solved to obtain equations for the free ligand  $[L]$  or free metal concentration  $[M]$ . The expected fluorescence intensity of solution is given by<sup>14,15</sup>  $F_T = \sum \alpha_i F_i$ , where  $\alpha_i$  and  $F_i$  are the molar fraction and fluorescence intensity of the involved species, respectively. For evaluation of the stepwise stability constants from the fluorescence intensity vs  $M^{II}/L$  molar ratio data, the nonlinear least-squares curve-fitting program KINFIT was used.<sup>16</sup> The program is based on the iterative adjustment of calculated values of fluorescence intensity to the observed values by using the Wentworth matrix technique<sup>17</sup> or the Pawell procedure.<sup>18</sup> Adjustable parameters are the stepwise stability constants

(14) Pistolis, G.; Malliaris, A. *J. Phys. Chem.* **1996**, *100*, 15562.

(15) Eddaoudi, M.; Coleman, A. W.; Prognon, P.; Lopez-Mabia, P. *J. Chem. Soc., Perkin Trans. 2* **1996**, 955.

(16) Nicely, V. A.; Dye, J. L. *J. Chem. Educ.* **1971**, *48*, 443.

(17) Wentworth, W. E. *J. Chem. Educ.* **1962**, *42*, 96 and 162.

(18) Pawell, M. J. D. *Comput. J.* **1964**, *7*, 155.

of the complexes present in solution and the corresponding fluorescence intensities depending on the model adopted.

The free metal ion, [M] (for models I and III), or free ligand concentrations, [L] (for model II), were calculated by means of a Newton–Raphson procedure. Once the values of either [M] or [L] had been obtained, the value of fluorescence intensity was calculated from the corresponding equations for  $F_T$ , by using the estimated values of the stability constants at the current iteration step of the program. Refinement of the parameters was continued until the sum-of-squares of the residuals between calculated and observed values of the fluorescence intensity for all experimental points were minimized. The output of the program KINFIT comprises the refined parameters, the sum-of-squares, and the standard deviation of the data.

**Crystallography.** Single-crystal data collection for [Pb(L<sup>1</sup>)]-[ClO<sub>4</sub>]<sub>2</sub>·1/2H<sub>2</sub>O (**1**) was performed on a Bruker SMART CCD diffractometer using  $\omega$  scans. For [Pb(L<sup>2</sup>)]-[ClO<sub>4</sub>]<sub>2</sub>·MeNO<sub>2</sub> (**1a**), [Pb(L<sup>3</sup>)<sub>2</sub>]-[ClO<sub>4</sub>]<sub>2</sub>·2MeCN (**1b**), and [Cd(L<sup>3</sup>)]-[NO<sub>3</sub>]<sub>2</sub> (**2b**) data were acquired on an Enraf Nonius CAD4 diffractometer using  $\omega$  scans. All data sets were corrected for Lorentz–polarization effects and for absorption. The structures were solved by direct methods using SHELXS 86,<sup>19</sup> and full-matrix least-squares refinements on  $F^2$  were performed using SHELXL 93.<sup>20</sup> All non-H atoms were refined anisotropically, and H atoms were placed at geometrical positions and thereafter allowed to ride on their parent atoms. In **1b** one of the two ClO<sub>4</sub><sup>−</sup> counteranions was found to be disordered for three of its oxygen atoms across a mirror plane. The disorder was modeled setting the occupancy of each disordered site to 0.5. In **1b**, atoms C(15) and C(16) display slightly high displacement parameters which might be indicative of partial disorder due to the presence of similar but different conformations for the aliphatic portion of the macrocyclic ligand. However, any attempt to split these atoms into two components offered no advantage. The H atoms of the water molecule in **1** and of the acetonitrile molecules in **1b** could not be positioned reliably.

## Results and Discussion

**Solution Studies.** As with other phenanthroline derivatives used as fluorescent chemosensors,<sup>21</sup> the absorption and fluorescence emission spectra of L<sup>1</sup>–L<sup>3</sup> in MeCN show an absorption band at about 280 nm and a fluorescent band around 360 nm (Figure 1). Generally, the Lewis base–acid interaction of the phenanthroline nitrogen atoms with positively charged species (H<sup>+</sup> or metal ions) decreases the intensity of the fluorescence emission due to a consequent stabilization of the weak emissive <sup>1</sup>n $\pi^*$  singlet excited state with respect to the strong emissive <sup>1</sup> $\pi\pi^*$  one.<sup>9,12</sup> However, for some 2,9-dialkylated 1,10-phenanthroline derivatives, a marked and selective increase in the fluorescence emission intensity was observed in the presence of lithium ions.<sup>22</sup> This effect was concluded to be a consequence of the rigidity imposed on the fluorophore by strong complexation with a consequent decrease in the nonradiative rate constant.<sup>22</sup>

To evaluate whether L<sup>1</sup>–L<sup>3</sup> could be used as fluorescent chemosensors for Pb<sup>II</sup>, Cd<sup>II</sup>, and Hg<sup>II</sup>, we recorded the fluorescence spectra variations that occur upon addition of increasing amounts of each of these three metals to an acetonitrile solution of L<sup>1</sup>, L<sup>2</sup>, or L<sup>3</sup> at 25 °C. The shape and position of the fluorescence emission bands do not change in the presence of M<sup>II</sup> (M = Pb, Cd, or Hg) compared to those of free L<sup>1</sup>–L<sup>3</sup>, whereas the emission intensities change as a function of the M<sup>II</sup>/L (L = L<sup>1</sup>, L<sup>2</sup>, L<sup>3</sup>) molar ratio according to the curves reported in Figure 2. It should be noted that because of the very short fluorescence lifetimes reported for polypyridine ligands and their complexes (10–100 ns),<sup>23</sup> and the low concentration conditions used in this study, the effect of concentration quenching should be negligible.

A chelation enhancement of quenching of the fluorescence (CHEQ effect) is observed for all three ligands on addition of increasing quantities of Pb<sup>II</sup> or Hg<sup>II</sup>. In the case of L<sup>3</sup>, the CHEQ effect due to addition of Pb<sup>II</sup> is remarkably pronounced compared to that observed on adding Hg<sup>II</sup>. From the inflection points in the fluorescence intensity/molar ratio plots (Figure 2a,b), it can be inferred that 1:1 [Pb(L)]<sup>2+</sup> and [Hg(L)]<sup>2+</sup> (L = L<sup>1</sup>, L<sup>2</sup>) complex cations are formed in acetonitrile solution. The formation of [M(L)<sub>2</sub>]<sup>2+</sup> species appears to take place only with L<sup>3</sup> for M = Pb<sup>II</sup> (Figure 2c; in this case it appears that the [Pb(L<sup>3</sup>)<sub>2</sub>]<sup>2+</sup> species is the only one formed upon addition of Pb<sup>II</sup> to L<sup>3</sup>) and with both L<sup>1</sup> and L<sup>2</sup> (Figure 2a,b) for M = Hg<sup>II</sup> (in some cases the inflection points are not neat, but the stoichiometry of the corresponding complex species has also been confirmed by the best fitting of the experimental data with the appropriate complexation models and by conductometric measurements; see later). The trend of the fluorescence intensity variation observed upon addition of Cd<sup>II</sup> to acetonitrile solutions of L<sup>1</sup>, L<sup>2</sup>, or L<sup>3</sup> is quite different from that recorded in the case of Pb<sup>II</sup> and Hg<sup>II</sup>. In fact, a CHEQ effect is observed with L<sup>1</sup> and L<sup>3</sup> up to Cd<sup>II</sup>/L molar ratios of 1 and 0.5, respectively (the CHEQ effect recorded in the case of L<sup>3</sup> is very low compared to that observed on adding Pb<sup>II</sup>, Figure 2c). For higher molar ratios a chelation enhancement of fluorescence (CHEF effect) is then observed until a Cd<sup>II</sup>/L molar ratio of 2 and 1 is reached for L<sup>1</sup> and L<sup>3</sup>, respectively (Figure 2a,c). The shape of the spectrofluorometric titration curves suggests formation of the species [Cd(L<sup>1</sup>)]<sup>2+</sup> and [Cd<sub>2</sub>(L<sup>1</sup>)]<sup>4+</sup> during addition of Cd<sup>II</sup> to L<sup>1</sup> and the species [Cd(L<sup>3</sup>)]<sup>2+</sup> and [Cd-(L<sup>3</sup>)<sub>2</sub>]<sup>2+</sup> during titration of L<sup>3</sup>. The spectrofluorometric titration curve of L<sup>2</sup> with Cd<sup>II</sup> in acetonitrile solution shows a CHEF effect throughout the whole range of Cd<sup>II</sup>/L<sup>2</sup> molar ratios explored with inflection points at Cd<sup>II</sup>/L<sup>2</sup> values of 0.5 and 1, which indicate the formation in solution of the species [Cd(L<sup>2</sup>)]<sup>2+</sup> and [Cd(L<sup>2</sup>)<sub>2</sub>]<sup>2+</sup>.

To further investigate the stoichiometry of the complex species formed during the spectrofluorometric titrations, the molar conductance of acetonitrile solutions of Pb<sup>II</sup>, Hg<sup>II</sup>, or Cd<sup>II</sup> was monitored at 25 ± 0.1 °C while adding increasing amounts of the macrocyclic ligands. The resulting molar

(19) Sheldrick, G. M. SHELXS 86. *Acta Crystallogr., Sect. A* **1990**, *46*, 467.

(20) Sheldrick, G. M. SHELXL 93; University of Göttingen: Göttingen, Germany, 1993.

(21) Armaroli, N.; De Cola, L.; Balzani, V.; Sauvage, J.-P.; Dietrich-Buchecker, C. O.; Kern, J.-M. *J. Chem. Soc., Faraday Trans.* **1992**, *553*.

(22) (a) Hiratani, K.; Nomoto, M.; Sugihara, H.; Okada, T. *Analyst* **1992**, *117*, 1491. (b) Hiratani, K.; Nomoto, M.; Sugihara, H.; Okada, T. *Chem. Lett.* **1990**, 43.

(23) Creutz, C.; Chou, M.; Netzel, T. L.; Okamura, M.; Sutin, N. *J. Am. Chem. Soc.* **1980**, *102*, 1309.

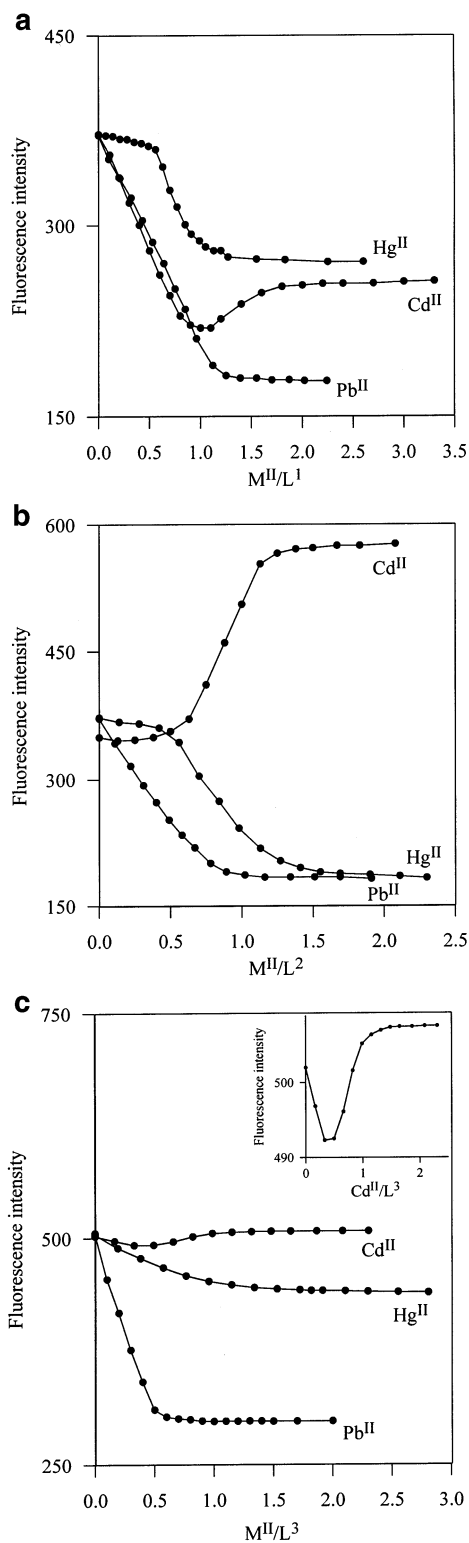


**Figure 2.** Fluorescence intensity–molar ratio plots for  $L^1$  (a),  $L^2$  (b), and  $L^3$  (c) ( $1.0 \times 10^{-5}$  M, MeCN, 25 °C) in the presence of increasing amounts of  $Pb^{II}$ ,  $Hg^{II}$ , and  $Cd^{II}$ . Inset to (c): Enlargement of the fluorescence intensity–molar ratio plot for the titration of  $L^3$  with  $Cd^{II}$ .

conductance/molar ratio plots are shown in Figure 3 for the  $Pb^{II}$  and  $Cd^{II}$  cases. While  $L^1$ – $L^3$  solutions possess a negligible conductance, their addition to both metal ion solutions causes a rather large continuous increase in molar conductance. This could be due to a lower mobility of the solvated metal ion and/or to the existence of ion pairing in

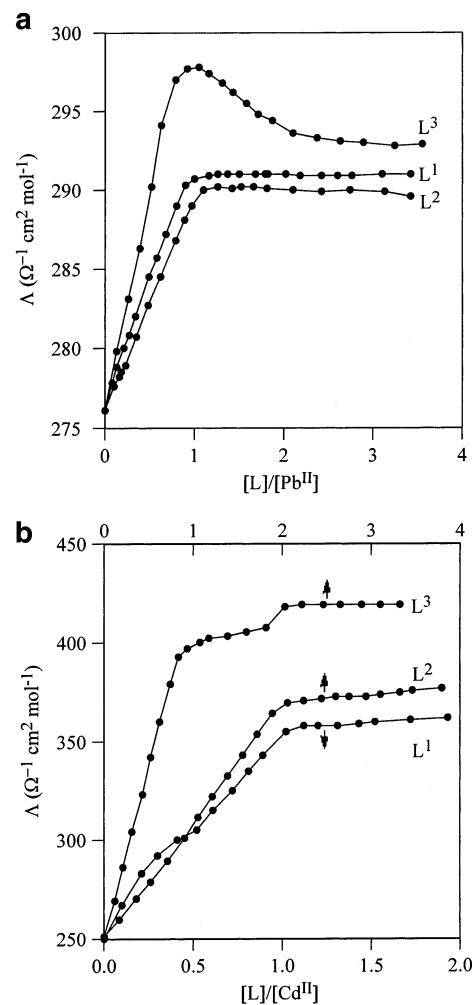


**Figure 3.** (a) Molar conductance vs  $[L]/[Pb^{II}]$  in acetonitrile at 25 °C:  $L = L^1$  ( $[Pb^{II}] = 4.5 \times 10^{-5}$  M);  $L = L^2$  ( $[Pb^{II}] = 7.75 \times 10^{-5}$  M);  $L = L^3$  ( $[Pb^{II}] = 7.0 \times 10^{-5}$  M). (b) Molar conductance vs  $[L]/[Cd^{II}]$  in acetonitrile at 25 °C:  $L = L^1$  ( $[Cd^{II}] = 3.6 \times 10^{-5}$  M);  $L = L^2$  ( $[Cd^{II}] = 7.2 \times 10^{-5}$  M);  $L = L^3$  ( $[Cd^{II}] = 7.2 \times 10^{-5}$  M). Arrows indicate the abscissa to which the plots refer.

the initial solution of the metal salt.<sup>24</sup> From Figure 3 it is clear that the molar conductance/molar ratio plots possess distinct inflection points at molar ratios that exactly confirm the formation of the aforementioned  $Pb^{II}$  and  $Cd^{II}$  complex species with the three ligands (in Figure 3b, a change in the slope can be recognized on a careful look at the conductance/molar ratio plot at the  $L^2/Cd^{II}$  molar ratio of 1). The conductometric data in the case of  $Pb^{II}$  and  $L^3$  (Figure 3a) also indicate presence of the 1:1  $[Pb(L^3)]^{2+}$  species whose formation was not highlighted by the spectrofluorometric data (Figure 2c). However, in the case of  $Hg^{II}$ , the change in molar conductance with the ligand-to-cation molar ratio revealed some unexpected and unreproducible fluctuations with no clear-cut evidence for the exact stoichiometry of the macrocycle– $Hg^{II}$  complexes.

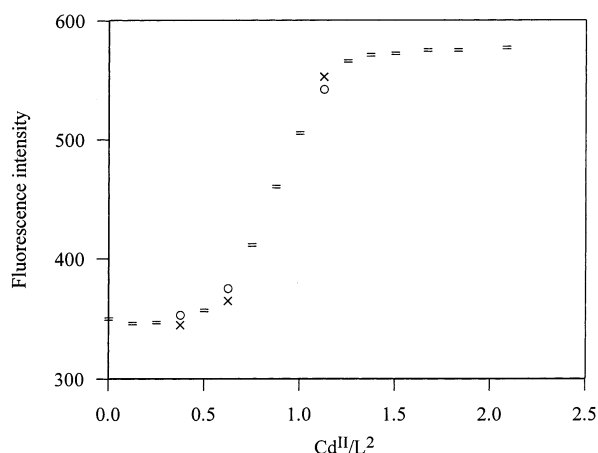
The stepwise formation constants of the complex species resulting from the spectrofluorometric titrations were evalu-

(24) (a) Amini, M. K.; Shamsipur, M. *Inorg. Chim. Acta* **1991**, *183*, 65. (b) Pourghobadi, Z.; Seyyed-Majidi, F.; Daghighi-Asli, M.; Parsa, F.; Moghimi, A.; Ganjali, M. R.; Aghabozorg, H.; Shamsipur, M. *Pol. J. Chem.* **2000**, *74*, 837.

**Table 1.** Stepwise Formation Constants<sup>a</sup> of Pb<sup>II</sup>, Cd<sup>II</sup>, and Hg<sup>II</sup> Complexes with L<sup>1</sup>–L<sup>3</sup> in Acetonitrile at 25 °C Calculated by Fitting the Fluorescence/Molar Ratio Data

| ligand         | metal ion        | log K <sub>1</sub> <sup>b</sup> | log K <sub>2</sub> <sup>c</sup> |
|----------------|------------------|---------------------------------|---------------------------------|
| L <sup>1</sup> | Pb <sup>II</sup> | 7.5(0.2)                        |                                 |
|                | Cd <sup>II</sup> | 5.53(0.02)                      | 2.62(0.03) <sup>d</sup>         |
|                | Hg <sup>II</sup> | 5.95(0.16)                      | 2.93(0.12)                      |
| L <sup>2</sup> | Pb <sup>II</sup> | 6.24(0.05)                      |                                 |
|                | Cd <sup>II</sup> | 6.40(0.09)                      | 3.00(0.09)                      |
|                | Hg <sup>II</sup> | 5.34(0.15)                      | 2.69(0.12)                      |
| L <sup>3</sup> | Pb <sup>II</sup> | 6.07(0.06)                      | 2.22(0.06) <sup>e</sup>         |
|                | Cd <sup>II</sup> | 5.86(0.04)                      | 2.91(0.03)                      |
|                | Hg <sup>II</sup> | 5.56(0.04)                      |                                 |

<sup>a</sup> Value in parentheses indicate standard deviations. <sup>b</sup> M + L ⇌ ML. <sup>c</sup> ML + L ⇌ ML<sub>2</sub>. <sup>d</sup> This value refers to the formation constant of the [Cd<sub>2</sub>(L<sup>1</sup>)<sup>4+</sup>] complex: ML + M ⇌ M<sub>2</sub>L. <sup>e</sup> Using only a 1:2 complexation model to fit the experimental data (M + 2L ⇌ ML<sub>2</sub>), we calculated a value of 7.8 ± 0.6 for log K with a considerable increase of the sum of the squared errors in the fitting of the experimental data (from 56.9 to 891.3).

**Figure 4.** Computer fit of the fluorescence intensity/molar ratio data obtained from the titration of L<sup>2</sup> with Cd<sup>II</sup> in MeCN solution: (x) calculated points; (o) experimental points; (=) experimental and calculated points the same within the resolution of the plot.

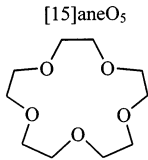
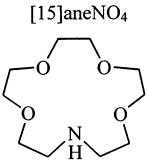
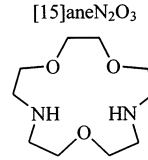
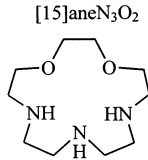
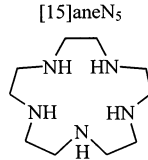
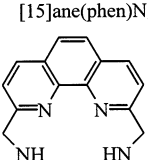
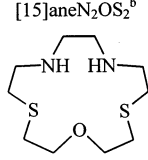
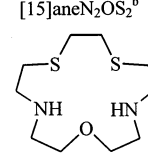
ated by fitting the fluorescence/molar ratio data to the proper models using a nonlinear least-squares curve-fitting program (see Experimental Section), and the results are summarized in Table 1. All computer fits of the fluorescence intensity/molar ratio data have been deposited as Supporting Information; an example is shown in Figure 4. The data related to the spectrofluorometric titration of L<sup>3</sup> with Pb<sup>II</sup> were fitted according to both 1:2 (M + 2L ⇌ ML<sub>2</sub>) and 1:1 + 1:2 (M + L ⇌ ML; ML + L ⇌ ML<sub>2</sub>) complexation models. The results clearly indicate the latter to be the best model (Table 1) with formation of the [Pb(L<sup>3</sup>)<sup>2+</sup>] intermediate species according to the conductometric data. The stability constants for the 1:1 complexes of the three metal ions with the three ligands are of the same order of magnitude. In the case of Pb<sup>II</sup> a slight decrease in K<sub>1</sub> is observed on passing from L<sup>1</sup> to L<sup>3</sup>, while a similar trend is not observed for Cd<sup>II</sup> and Hg<sup>II</sup>. The formation constants K<sub>2</sub> for [ML<sub>2</sub>]<sup>2+</sup> species (M = Hg<sup>II</sup>, L = L<sup>1</sup>, L<sup>2</sup>; M = Pb<sup>II</sup>, L = L<sup>3</sup>; M = Cd<sup>II</sup>, L = L<sup>2</sup>, L<sup>3</sup>) are much lower than those calculated for the 1:1 complexes with log K<sub>2</sub> ranging from 3.00(9) to 2.22(6). In the case of Cd<sup>II</sup> and only with L<sup>1</sup> the 2:1 [Cd<sub>2</sub>(L<sup>1</sup>)<sup>4+</sup>] species seems to form in solution with log K<sub>2</sub> = 2.62(3). Two-to-one M<sub>2</sub>L complexes with macrocyclic ligands are quite rare

in the literature; for example, they are reported to form in MeOH solution between Pb<sup>II</sup> and Cd<sup>II</sup> and the macrocyclic ligands [15]aneN<sub>2</sub>O<sub>3</sub> (4,7,13-trioxa-1,10-diazacyclopentadecane)<sup>25a</sup> and [18]aneN<sub>2</sub>O<sub>4</sub> (4,7,13,16-tetraoxa-1,10-diazacyclooctadecane).<sup>25b</sup>

The investigation of structure–function relationships in the interaction of transition and post-transition metal ions with structural related macrocycles incorporating mixed donor atoms is of paramount importance for the design of new ligands with increased selectivity. In this respect Table 2 shows the O,N,S-mixed donor [15]ane pentadentate macrocycles for which, to the best of our knowledge, the complex formation with lead(II), cadmium(II), or mercury(II) has been investigated. The following discussion will be restricted to Pb<sup>II</sup> since only for this metal ion has the formation constant been calculated for the 1:1 complex with all the ligands (Table 2). As expected, the stability constants are strongly affected by the donor atom set. In particular, a strong dependence of log K for Pb<sup>II</sup> 1:1 complexes on the number of nitrogen atoms present in the macrocyclic frameworks is observed. The substitution of a nitrogen atom with either oxygen or sulfur in the ring cavity causes a dramatic decrease in the stability constant compared to [15]aneN<sub>5</sub>; this is in agreement with the “borderline” classification of Pb<sup>II</sup> in the scale of “hard” and “soft” acids. A similar trend, finely tuned by ring-size factors, was observed by Lindoy et al. on studying an extended range of 16- to 19-membered dibenzo-substituted pentadentate macrocycles containing oxygen, nitrogen, and sulfur donor atoms.<sup>6,32</sup> Interestingly, the stability constant for the 1:1 Pb<sup>II</sup> complex with the N<sub>5</sub>-donor ring containing a polyamine chain linking the 2,9-phenanthroline positions is significantly higher than that of the complex with [15]aneN<sub>5</sub> containing the same number of nitrogen donors. According to Bencini et al.,<sup>5a</sup> the reason for this enhancement in thermodynamic stability is a better coordination ability of the heteroaromatic nitrogens of the phenanthroline subunit toward lead(II). The same effect though is not observed on passing from both the [15]aneN<sub>2</sub>OS<sub>2</sub> ligands to L<sup>2</sup>. At the moment no hypothesis can be made to explain this behavior considering that the stability constants for Pb<sup>II</sup> with L<sup>1</sup>–L<sup>3</sup> and the ligands reported in Table 2, in particular the two [15]aneN<sub>2</sub>OS<sub>2</sub> macrocycles, have been determined in different solvents (MeCN for the former and water for the

- (25) (a) Spiess, B.; Arnaud-Neu, F.; Schwing-Weill, M. *Helv. Chim. Acta* **1980**, *63*, 2287. (b) Kulstad, S.; Malmsten, L. *J. Inorg. Nucl. Chem.* **1980**, *42*, 1193.
- (26) Buschmann, H.-J. *Inorg. Chim. Acta* **1985**, *98*, 43.
- (27) Byriel, K.; Dunster, K. R.; Gahan, L. R.; Kennard, C. H. L.; Latten, J. L.; Swann, I. L. *Polyhedron* **1992**, *11*, 1205.
- (28) Byriel, K.; Dunster, K. R.; Gahan, L. R. *Inorg. Chim. Acta* **1993**, *205*, 191.
- (29) Hancock, R.; Bhavan, R.; Wade, P. *Inorg. Chem.* **1989**, *28*, 187.
- (30) Kodama, M.; Kimura, E. *J. Chem. Soc., Dalton Trans.* **1978**, 1081.
- (31) Arnaud-Neu, F.; Schwing-Weill, M.-J.; Louis, R.; Weiss, R. *Inorg. Chem.* **1979**, *18*, 2956.
- (32) (a) Davis, C. A.; Leong, A. J.; Lindoy, L. F.; Kim, J.; Lee, S.-H. *Aust. J. Chem.* **1998**, *51*, 189. (b) Adam, K. R.; Arshad, S. P. H.; Baldwin, D. S.; Duckworth, P. A.; Leong, A. J.; Lindoy, L. F.; McCool, B. J.; McPartlin, M.; Taylor, B. A.; Tasker, P. A. *Inorg. Chem.* **1994**, *33*, 1194.

**Table 2.** Formation Constants for 1:1 Complexes between Pb<sup>II</sup>, Cd<sup>II</sup>, and Hg<sup>II</sup> with Mixed-Donor [15]ane Pentadentate Macrocycles<sup>a</sup>

|    |   |   |   |  |   |
|----|---|---|---|--|---|
|    |  |  |  |  |   |
| Pb | 3.92(MeOH) <sup>26</sup>  | 6.0(MeOH) <sup>27</sup>   | 7.87(MeOH) <sup>25a</sup>   |  |   |
| Cd |   |   | 8.72(MeOH) <sup>25a</sup>   |  |   |
| Hg |   | 10.3(MeOH) <sup>28</sup>  |   |  |   |
|    |  |  |  |  |  |
| Pb | 10.07(H <sub>2</sub> O) <sup>29</sup>   | 17.3(H <sub>2</sub> O) <sup>30</sup>  | 18.70(H <sub>2</sub> O) <sup>5a</sup>   | 6.78(H <sub>2</sub> O) <sup>31</sup>   | 5.67(H <sub>2</sub> O) <sup>31</sup>  |
| Cd | 10.05(H <sub>2</sub> O) <sup>29</sup>   | 19.2(H <sub>2</sub> O) <sup>30</sup>  |   | 7.13(H <sub>2</sub> O) <sup>31</sup>   | 6.53(H <sub>2</sub> O) <sup>31</sup>  |
| Hg |   | 28.5(H <sub>2</sub> O) <sup>30</sup>  |   |  |   |

<sup>a</sup> Solvent used in parentheses. <sup>b</sup> The same notation [15]aneN<sub>2</sub>OS<sub>2</sub> has been used for the two macrocycles 1-oxa-4,13-dithia-7,10-diazacyclopentadecane and 1-oxa-4,13-diaza-7,10-dithiacyclopentadecane characterized by a different arrangement of the donor atoms in the macrocyclic framework.

latter). Unfortunately, for solubility reasons, it was not possible to study in water the complexation reactions of L<sup>1</sup>–L<sup>3</sup>.

**Crystal Structures of [Pb(L<sup>1</sup>)] [ClO<sub>4</sub>]<sub>2</sub>·1/2H<sub>2</sub>O (1), [Pb(L<sup>2</sup>)] [ClO<sub>4</sub>]<sub>2</sub>·MeNO<sub>2</sub> (1a), [Pb(L<sup>3</sup>)<sub>2</sub>] [ClO<sub>4</sub>]<sub>2</sub>·2MeCN (1b), and [Cd(L<sup>3</sup>)] [NO<sub>3</sub>]<sub>2</sub> (2b).** The complexation ability of L<sup>1</sup>–L<sup>3</sup> toward Pb<sup>II</sup>, Cd<sup>II</sup>, and Hg<sup>II</sup> has also been investigated in the solid state. Whatever the M/L molar ratio used (1:1 or 1:2), the reaction between L<sup>1</sup>–L<sup>3</sup> and Cd<sup>II</sup> and Hg<sup>II</sup> always resulted in 1:1 complexes, as demonstrated by elemental analysis and FAB mass spectroscopy (see Experimental Section). In the case of Pb<sup>II</sup>, 1:1 complexes were always isolated with L<sup>1</sup> and L<sup>2</sup>, whereas the only compound obtained with L<sup>3</sup> in the solid state had a formulation corresponding to a 1:2 Pb/L<sup>3</sup> stoichiometry. Crystals suitable for X-ray structural analysis were obtained for the complexes [Pb(L<sup>1</sup>)] [ClO<sub>4</sub>]<sub>2</sub>·1/2H<sub>2</sub>O (1), [Pb(L<sup>2</sup>)] [ClO<sub>4</sub>]<sub>2</sub>·MeNO<sub>2</sub> (1a), [Pb(L<sup>3</sup>)<sub>2</sub>] [ClO<sub>4</sub>]<sub>2</sub>·2MeCN (1b), and [Cd(L<sup>3</sup>)] [NO<sub>3</sub>]<sub>2</sub> (2b).

In **1** two perchlorate ions and a water molecule bridge two symmetry-related [Pb(L<sup>1</sup>)]<sup>2+</sup> units to form a binuclear species, as shown in Figure 5. Each Pb<sup>II</sup> in the dimer interacts with a further perchlorate ion acting as a monodentate ligand so to reach an overall nine-coordination. The bonds to the donor atoms are evenly distributed about the coordination sphere; but some are significantly longer than others (Table 3). In particular, the two N-donors from the phenanthroline unit of the macrocyclic ligand are more strongly coordinated to the metal centers with bond lengths of 2.582(3) and 2.572(3) Å, respectively, while the three S-donors from the L<sup>1</sup> molecule and the four O-donors from the perchlorate ions and the water molecule are at rather longer distances ranging from 2.852(3) [Pb–O(5)] to 3.105(5) Å [Pb–O(6')] (Table 3). The Pb–N bond lengths are comparable to the usually observed Pb–N<sub>pyridine</sub> distances,<sup>7a,33</sup> and the same can be said

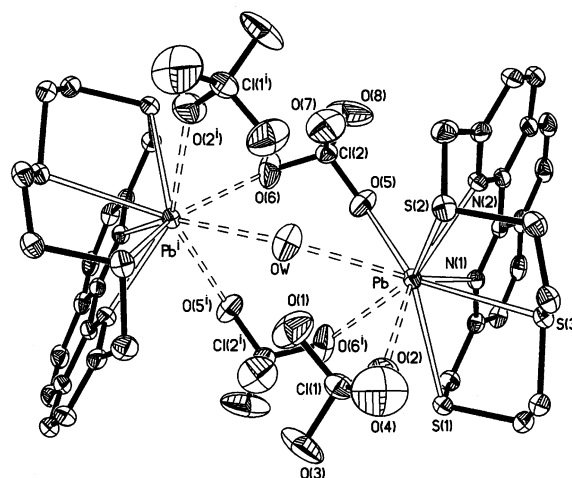


**Figure 5.** View of the [Pb(L<sup>1</sup>)] [ClO<sub>4</sub>]<sub>2</sub>·1/2H<sub>2</sub>O (1) in its dimeric form with the adopted numbering scheme. Displacement ellipsoids are drawn at 30% probability, and hydrogen atoms are omitted for clarity (i, 1 – x, y, 1/2 – z).

of the Pb–S distances in comparison with those observed in the macrocyclic lead(II) complexes containing Pb–S<sub>thioether</sub> bonds located in the files of the Cambridge Crystallographic data Centre.<sup>7a,33,34</sup> The Pb–O distances are significantly longer than those normally found for O-donating counteranions coordinated to lead(II), and they should be better considered as long contacts,<sup>7a,33,34</sup> in fact, except for Pb–O(5), they are also longer than the estimated sum of the Shannon ionic radius of nine-coordinate lead(II) (1.35 Å)<sup>35</sup> and the van der Waals radius of oxygen (1.50 Å).<sup>36</sup> In this

(33) (a) Bashall, A.; McPartlin, M.; Murphy, B. P.; Fenton, D. E.; Kitchen, S. J.; Tasker, P. A. *J. Chem. Soc., Dalton Trans.* **1990**, 505. (b) Constable, E. C.; Sacht, C.; Palo, G.; Tocher, D. A.; Truter, M. R. *J. Chem. Soc., Dalton Trans.* **1993**, 1307 and references therein.

(34) Blake, A. J.; Fenske, D.; Li, W.-S.; Lippolis, V.; Schröder, M. *J. Chem. Soc., Dalton Trans.* **1998**, 3961.

(35) Shannon, R. D. *Acta Crystallogr., Sect. A* **1976**, 32, 751.

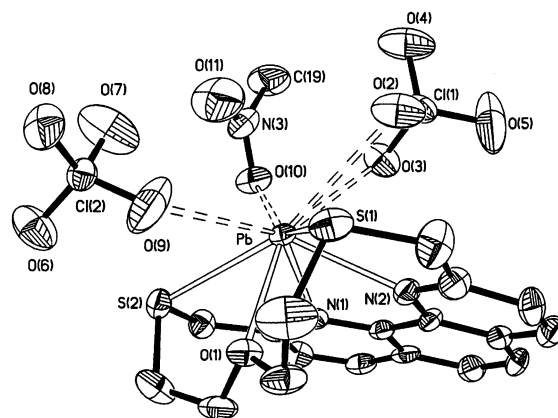
**Table 3.** Selected Bond Lengths (Å) and Angles (deg) for [Pb(L<sup>1</sup>)][(ClO<sub>4</sub>)<sub>2</sub>·<sup>1</sup>/<sub>2</sub>H<sub>2</sub>O (1)<sup>a</sup>

|                            |            |                            |            |
|----------------------------|------------|----------------------------|------------|
| Pb–N(1)                    | 2.582(3)   | Pb–N(2)                    | 2.572(3)   |
| Pb–S(1)                    | 3.0156(10) | Pb–S(2)                    | 3.0185(10) |
| Pb–S(3)                    | 2.9832(9)  | Pb–Ow                      | 2.995(3)   |
| Pb–O(5)                    | 2.852(3)   | Pb–O(2)                    | 2.967(4)   |
| Pb–O(6 <sup>i</sup> )      | 3.105(5)   |                            |            |
| S(1)–Pb–N(1)               | 67.23(7)   | S(1)–Pb–N(2)               | 126.70(7)  |
| S(1)–Pb–S(2)               | 130.60(3)  | S(1)–Pb–S(3)               | 69.39(3)   |
| S(1)–Pb–Ow                 | 124.04(3)  | S(1)–Pb–O(5)               | 115.99(7)  |
| S(1)–Pb–O(2)               | 70.84(8)   | S(1)–Pb–O(6 <sup>i</sup> ) | 61.37(8)   |
| S(2)–Pb–N(1)               | 126.83(7)  | S(2)–Pb–N(2)               | 67.38(7)   |
| S(2)–Pb–S(3)               | 70.08(3)   | S(2)–Pb–Ow                 | 71.98(9)   |
| S(2)–Pb–O(5)               | 112.93(7)  | S(2)–Pb–O(2)               | 73.44(9)   |
| S(2)–Pb–O(6 <sup>i</sup> ) | 150.53(7)  | S(3)–Pb–N(1)               | 76.07(6)   |
| S(3)–Pb–N(2)               | 76.47(7)   | S(3)–Pb–Ow                 | 135.49(10) |
| S(3)–Pb–O(5)               | 138.21(8)  | S(3)–Pb–O(2)               | 76.81(8)   |
| S(3)–Pb–O(6 <sup>i</sup> ) | 130.63(8)  | N(1)–Pb–N(2)               | 65.61(9)   |
| N(1)–Pb–Ow                 | 147.60(11) | N(1)–Pb–O(5)               | 69.82(9)   |
| N(1)–Pb–O(2)               | 135.81(10) | N(1)–Pb–O(6 <sup>i</sup> ) | 81.99(9)   |
| N(2)–Pb–Ow                 | 109.08(7)  | N(2)–Pb–O(5)               | 67.97(10)  |
| N(2)–Pb–O(2)               | 138.10(11) | N(2)–Pb–O(6 <sup>i</sup> ) | 131.74(10) |
| O(5)–Pb–Ow                 | 78.56(11)  | O(5)–Pb–O(2)               | 144.97(11) |
| O(5)–Pb–O(6 <sup>i</sup> ) | 67.70(11)  | O(2)–Pb–O(6 <sup>i</sup> ) | 90.06(13)  |
| O(2)–Pb–Ow                 | 70.77(11)  | O(6 <sup>i</sup> )–Pb–Ow   | 79.64(11)  |

<sup>a</sup> Symmetry transformation used to generate equivalent atoms: (i) 1 – x, y, <sup>1</sup>/<sub>2</sub> – z.

structure, L<sup>1</sup> adopts a conformation very similar to that observed in related complexes with d<sup>8</sup> transition metal ions<sup>13</sup> while trying to encapsulate the metal ion within a cavity having a square-based pyramidal stereochemistry: the aliphatic chain is folded over the phenanthroline unit with the planes containing the aromatic and the aliphatic moieties, defined by the three S donors, forming a dihedral angle of 65.9(1)°. However, in this case L<sup>1</sup> is not able to fully accommodate lead(II) into its square-based pyramidal cavity. Each Pb<sup>II</sup> in the dimer is displaced 0.92 Å from the mean plane defined by the atoms N(1), N(2), S(1), and S(2) toward the O-donor manifold of the perchlorate ions and the water molecule with an interatomic metal–metal distance of 5.3796(5) Å. A similar conformational behavior of the ligand and arrangement of the donor atoms around the metal center has been observed by Bencini et al. for the lead(II) complex of the L<sup>1</sup> structural analogue, which has three secondary nitrogens instead of the sulfur donors.<sup>5a</sup> In this case both mononuclear and dinuclear seven-coordinate lead(II) species were present in the asymmetric unit with a single  $\mu$ -Br bridge between the two metal centers of the dinuclear species in order to reach a Pb···Pb interatomic distance of 5.618(1) Å.

On passage from L<sup>1</sup> to L<sup>2</sup> a mononuclear lead(II) complex is obtained in which a nine coordination at the metal center is apparently achieved via the five donor atoms of the macrocyclic ligand and four O-donors, three of the latter deriving respectively from one terminal bidentate and one monodentate ClO<sub>4</sub><sup>–</sup> ion and the fourth from a nitromethane molecule (Figure 6; Table 4). The Pb–N and Pb–S bond lengths are comparable to those observed in the [Pb(L<sup>1</sup>)]<sup>2+</sup> unit of the dimeric complex described above (Figure 5), whereas the Pb–O(1) distance [2.589(8) Å] is rather shorter than the corresponding Pb–S(3) one. The other Pb–O

**Figure 6.** View of the [Pb(L<sup>2</sup>)]<sup>2+</sup> cation with the adopted numbering scheme, interacting at the metal center with two ClO<sub>4</sub><sup>–</sup> anions and a nitromethane molecule (double dashed lines). Displacement ellipsoids are drawn at 30% probability, and hydrogen atoms are omitted for clarity.**Table 4.** Selected Bond Lengths (Å) and Angles (deg) for [Pb(L<sup>2</sup>)][(ClO<sub>4</sub>)<sub>2</sub>·MeNO<sub>2</sub> (1a)]

|               |            |               |           |
|---------------|------------|---------------|-----------|
| Pb–N(1)       | 2.540(8)   | Pb–N(2)       | 2.546(9)  |
| Pb–S(1)       | 2.981(3)   | Pb–S(2)       | 2.955(3)  |
| Pb–O(1)       | 2.589(8)   | Pb–O(2)       | 3.186(13) |
| Pb–O(3)       | 2.853(9)   | Pb–O(9)       | 3.16(2)   |
| Pb–O(10)      | 3.208(14)  |               |           |
| S(1)–Pb–N(1)  | 68.2(2)    | S(1)–Pb–N(2)  | 125.5(2)  |
| S(1)–Pb–S(2)  | 128.54(10) | S(1)–Pb–O(1)  | 67.3(2)   |
| S(1)–Pb–O(2)  | 159.5(3)   | S(1)–Pb–O(3)  | 125.2(2)  |
| S(1)–Pb–O(9)  | 75.7(3)    | S(1)–Pb–O(10) | 69.7(2)   |
| S(2)–Pb–N(1)  | 129.8(2)   | S(2)–Pb–N(2)  | 69.2(2)   |
| S(2)–Pb–O(1)  | 68.6(2)    | S(2)–Pb–O(2)  | 65.2(2)   |
| S(2)–Pb–O(3)  | 106.2(2)   | S(2)–Pb–O(9)  | 63.6(3)   |
| S(2)–Pb–O(10) | 155.6(2)   | N(1)–Pb–N(2)  | 65.6(3)   |
| N(1)–Pb–O(2)  | 116.9(3)   | N(1)–Pb–O(3)  | 78.8(3)   |
| N(1)–Pb–O(9)  | 139.8(4)   | N(1)–Pb–O(10) | 68.8(3)   |
| N(2)–Pb–O(2)  | 71.4(3)    | N(2)–Pb–O(3)  | 71.2(3)   |
| N(2)–Pb–O(9)  | 129.3(4)   | N(2)–Pb–O(10) | 116.1(3)  |
| O(1)–Pb–N(1)  | 82.8(3)    | O(1)–Pb–N(2)  | 79.7(3)   |
| O(1)–Pb–O(2)  | 131.6(3)   | O(1)–Pb–O(3)  | 150.0(3)  |
| O(1)–Pb–O(9)  | 67.1(4)    | O(1)–Pb–O(10) | 134.8(3)  |
| O(2)–Pb–O(3)  | 44.0(3)    | O(2)–Pb–O(9)  | 103.2(4)  |
| O(2)–Pb–O(10) | 93.1(3)    | O(3)–Pb–O(9)  | 138.9(4)  |
| O(3)–Pb–O(10) | 57.8(3)    | O(9)–Pb–O(10) | 114.5(4)  |

distances involving the two ClO<sub>4</sub><sup>–</sup> ligands and the MeNO<sub>2</sub> molecule still are considerably longer than those usually expected for oxygen-donating counteranions interacting with Pb<sup>II</sup>.<sup>7a,33b,34</sup> This structural feature, common to both the [Pb(L<sup>1</sup>)][(ClO<sub>4</sub>)<sub>2</sub>·<sup>1</sup>/<sub>2</sub>H<sub>2</sub>O (1) and [Pb(L<sup>2</sup>)][(ClO<sub>4</sub>)<sub>2</sub>·MeNO<sub>2</sub> (1a)] structures, might be indicating the presence in the two compounds of a stereochemically active 6s<sup>2</sup> lone pair positioned in the coordination hemisphere left free by the macrocyclic ligands. The conformational behavior of L<sup>2</sup> upon coordination to Pb<sup>II</sup> is similar to that observed for L<sup>1</sup>, and also in [Pb(L<sup>2</sup>)][(ClO<sub>4</sub>)<sub>2</sub>·MeNO<sub>2</sub> (Figure 6) the Pb<sup>II</sup> ion is “perching” above the macrocyclic cavity of L<sup>2</sup> rather than “nesting” within it: it is displaced 0.91 Å out of the main plane defined by the atoms N(1), N(2), S(1), and S(2) in the opposite direction of the Pb–O(1) vector.

The reaction of Pb(ClO<sub>4</sub>)<sub>2</sub>·4H<sub>2</sub>O with 0.5 molar equiv of L<sup>3</sup> in refluxing MeOH for 1 h gave well-shaped colorless crystals after removal of the solvent and recrystallization of the resulting white product from MeCN/MeNO<sub>2</sub> by diffusion of Et<sub>2</sub>O. Elemental analysis suggested the formulation [Pb(L<sup>3</sup>)<sub>2</sub>][(ClO<sub>4</sub>)<sub>2</sub>·2MeCN (1b)] for the obtained crystals with a

(36) Pauling, L. *The Nature of Chemical Bond*, 3rd ed.; Cornell University Press: Ithaca, NY, 1960.



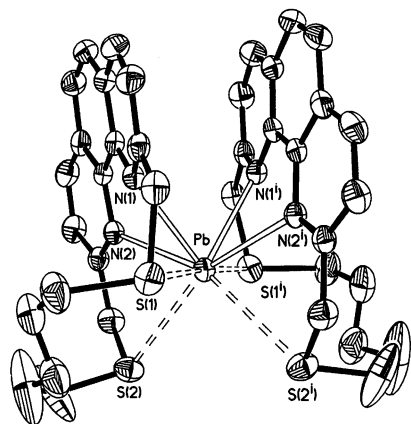


**Figure 7.** View of the  $[\text{Pb}(\text{L}^3)_2]^{2+}$  cation with the numbering scheme adopted. Displacement ellipsoids are drawn at 30% probability, and hydrogen atoms are omitted for clarity (i,  $1-x$ ,  $y$ ,  $1/2-z$ ).

**Table 5.** Selected Bond Lengths (Å) and Angles (deg) for  $[\text{Pb}(\text{L}^3)_2][\text{ClO}_4]_2 \cdot 2\text{MeCN}$  (**1b**)<sup>a</sup>

|                            |            |                            |           |
|----------------------------|------------|----------------------------|-----------|
| Pb–N(1)                    | 2.607(4)   | Pb–N(2)                    | 2.695(4)  |
| Pb–S(1)                    | 3.193(2)   | Pb–S(2)                    | 3.251(2)  |
| S(1)–Pb–N(1)               | 62.42(10)  | S(1)–Pb–N(2)               | 108.58(9) |
| S(1)–Pb–S(2)               | 105.25(5)  | S(2)–Pb–N(1)               | 113.52(9) |
| S(2)–Pb–N(2)               | 62.46(10)  | N(1)–Pb–N(2)               | 62.41(12) |
| N(1)–Pb–N(1 <sup>i</sup> ) | 74.4(2)    | N(1)–Pb–N(2 <sup>i</sup> ) | 83.14(12) |
| N(1)–Pb–S(1 <sup>i</sup> ) | 119.95(10) | N(1)–Pb–S(2 <sup>i</sup> ) | 130.20(9) |
| N(2)–Pb–N(2 <sup>i</sup> ) | 137.1(2)   | N(2)–Pb–S(1 <sup>i</sup> ) | 72.42(9)  |
| N(2)–Pb–S(2 <sup>i</sup> ) | 160.40(10) | S(1)–Pb–S(1 <sup>i</sup> ) | 177.40(7) |
| S(1)–Pb–S(2 <sup>i</sup> ) | 72.98(5)   | S(2)–Pb–S(2 <sup>i</sup> ) | 98.06(6)  |

<sup>a</sup> Symmetry transformation used to generate equivalent atoms: (i)  $1-x$ ,  $y$ ,  $1/2-z$ .

1:2  $\text{Pb}^{\text{II}}/\text{L}^3$  stoichiometric ratio. Interestingly, the same product was obtained using 1 molar equiv of  $\text{L}^3$  in the complexation reaction; therefore, a single-crystal structure determination was undertaken to ascertain the stereochemistry and ligation of this complex. The structure confirms the formation of the  $[\text{Pb}(\text{L}^3)_2]^{2+}$  cation (Figure 7; Table 5) in which the metal center is sandwiched between two symmetry-related molecules of  $\text{L}^3$ . An overall  $[4\text{N} + 4\text{S}]$  eight-coordination at lead(II) results with Pb–N bond distances longer than those observed in the 1:1 complexes with  $\text{L}^1$  and  $\text{L}^2$  but still typical of the interaction of lead with imine and pyridine nitrogens.<sup>7a,33</sup> The Pb–S bond distances also are slightly longer than those seen in **1** and **1a** and locate themselves on the upper end of the range of variability for the lead–thioether distances reported in the literature.<sup>7a,33b,34</sup> These structural features are in agreement with the fact that  $\text{Pb}^{\text{II}}$  in **1b** is by far the most displaced (1.55 Å) from the mean  $\text{N}_2\text{S}_2$  coordination plane compared to the complexes with  $\text{L}^1$  and  $\text{L}^3$ . The  $[\text{Pb}(\text{L}^3)_2]^{2+}$  cation represents a rare example of a sandwich complex for lead(II) with macrocyclic ligands and nicely supports the formation of 1:2 M/L ( $\text{M} = \text{Pb}^{\text{II}}, \text{Hg}^{\text{II}}, \text{Cd}^{\text{II}}$ ;  $\text{L} = \text{L}^1\text{--}\text{L}^3$ ) species in solution (see Table 1).

Figure 8 shows the structure of the complex  $[\text{Cd}(\text{L}^3)]\text{[NO}_3\text{]}_2$  (**2b**) obtained from the reaction of cadmium nitrate with 1 molar equiv of  $\text{L}^3$ . Selected bond distances and angles are given in Table 6. The  $\text{Cd}^{\text{II}}$  ion resides in a distorted cubic  $\text{N}_2\text{S}_2\text{O}_4$  environment, bound by the four donors of the macrocyclic ligand and by two almost symmetrical bidentate

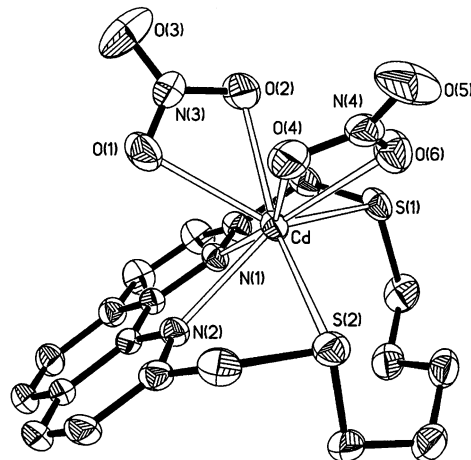


**Figure 8.** View of the  $[\text{Cd}(\text{L}^3)]\text{[NO}_3\text{]}_2$  (**2b**) complex with the adopted numbering scheme. Displacement ellipsoids are drawn at 30% probability, and hydrogen atoms are omitted for clarity.

**Table 6.** Selected Bond Lengths (Å) and Angles (deg) for  $[\text{Cd}(\text{L}^3)]\text{[NO}_3\text{]}_2$  (**2b**)

|              |            |              |            |
|--------------|------------|--------------|------------|
| Cd–N(1)      | 2.391(2)   | Cd–N(2)      | 2.393(2)   |
| Cd–S(1)      | 2.7455(10) | Cd–S(2)      | 2.8439(11) |
| Cd–O(1)      | 2.474(3)   | Cd–O(2)      | 2.451(2)   |
| Cd–O(4)      | 2.560(3)   | Cd–O(6)      | 2.450(2)   |
| S(1)–Cd–N(1) | 70.90(5)   | S(1)–Cd–N(2) | 129.00(5)  |
| S(1)–Cd–S(2) | 113.31(3)  | S(2)–Cd–N(1) | 124.36(5)  |
| S(2)–Cd–N(2) | 69.00(5)   | N(1)–Cd–N(2) | 68.55(7)   |
| N(1)–Cd–O(1) | 81.72(8)   | N(1)–Cd–O(2) | 84.78(9)   |
| N(1)–Cd–O(4) | 157.63(8)  | N(1)–Cd–O(6) | 144.41(8)  |
| N(2)–Cd–O(1) | 76.91(7)   | N(2)–Cd–O(2) | 124.19(7)  |
| N(2)–Cd–O(4) | 104.17(8)  | N(2)–Cd–O(6) | 145.53(8)  |
| S(1)–Cd–O(1) | 125.77(7)  | S(1)–Cd–O(2) | 80.43(6)   |
| S(1)–Cd–O(4) | 124.41(6)  | S(1)–Cd–O(6) | 75.17(6)   |
| S(2)–Cd–O(1) | 120.79(7)  | S(2)–Cd–O(2) | 150.07(7)  |
| S(2)–Cd–O(4) | 67.83(6)   | S(2)–Cd–O(6) | 79.02(7)   |
| O(1)–Cd–O(2) | 50.54(8)   | O(1)–Cd–O(4) | 75.98(9)   |
| O(1)–Cd–O(6) | 110.68(8)  | O(2)–Cd–O(4) | 82.42(9)   |
| O(2)–Cd–O(6) | 79.29(9)   | O(4)–Cd–O(6) | 49.76(8)   |

nitrate groups. The metal center is displaced out of the mean plane defined by the atoms N(1), N(2), S(1), and S(2) toward the  $\text{NO}_3^-$  ligands. The conformation adopted by  $\text{L}^3$  in this complex is very similar to that observed in the sandwich complex with  $\text{Pb}^{\text{II}}$ . This confirms the general conformational characteristic of this type of macrocycles of having the aliphatic portion of the ring folded over the phenanthroline unit.<sup>13</sup> In the case of pentadentate ligands such as  $\text{L}^1$  and  $\text{L}^2$  the donor atoms are preorganized to impose a square-based pyramidal coordination sphere at  $d^8$  transition metal centers. However, the ring cavity is not large enough to fully encapsulate larger  $d^{10}$  metal ions such as  $\text{Cd}^{\text{II}}$  and  $\text{Pb}^{\text{II}}$ . Crystal data and details of all four structure determinations appear in Table 7.

## Conclusions

The results reported in this paper clearly demonstrate the ability of the mixed donor macrocycles  $\text{L}^1\text{--}\text{L}^3$  containing a phenanthroline subunit to coordinate not only  $d^8$  transition metal ions but also  $d^{10}$  and main group metal ions. Since the phenanthroline group has fluorescence emission properties, these new macrocycles could be used as chemosensors for heavy metal ions by exploiting the quenching or enhancement effects on the fluorescence emission of the

**Table 7.** Crystallographic Data

|   | {[Pb(L <sup>1</sup> )][(ClO <sub>4</sub> ) <sub>2</sub> ]} <sub>2</sub> ·H <sub>2</sub> O ( <b>1</b> )        | [Pb(L <sup>2</sup> )][(ClO <sub>4</sub> ) <sub>2</sub> ]·MeNO <sub>2</sub> ( <b>1a</b> )        | [Pb(L <sup>3</sup> ) <sub>2</sub> ][(ClO <sub>4</sub> ) <sub>2</sub> ]·2MeCN ( <b>1b</b> )     | [Cd(L <sup>3</sup> )][(NO <sub>3</sub> ) <sub>2</sub> ] ( <b>2b</b> )          |
|---|---|---|--|--|
| formula                                 | C <sub>36</sub> H <sub>38</sub> Cl <sub>4</sub> N <sub>4</sub> O <sub>17</sub> Pb <sub>2</sub> S <sub>6</sub> | C <sub>19</sub> H <sub>21</sub> Cl <sub>2</sub> N <sub>3</sub> O <sub>11</sub> PbS <sub>2</sub> | C <sub>42</sub> H <sub>46</sub> Cl <sub>2</sub> N <sub>6</sub> O <sub>8</sub> PbS <sub>4</sub> | C <sub>19</sub> H <sub>20</sub> CdN <sub>4</sub> O <sub>6</sub> S <sub>2</sub> |
| M                                       | 1547.24   | 809.60  | 1169.18  | 576.91   |
| cryst system                            | monoclinic  | monoclinic  | monoclinic   | monoclinic   |
| space group                             | C2/c (No. 15)   | P2 <sub>1</sub> /n (No. 14)   | C2/c (No. 15)  | P2 <sub>1</sub> /n (No. 14)  |
| a/Å                                     | 19.396(2)   | 13.584(3)   | 15.081(5)  | 8.545(2)   |
| b/Å                                     | 18.412(2)   | 13.993(2)   | 22.270(6)  | 18.578(6)  |
| c/Å                                     | 13.785(1)   | 14.648(3)   | 13.862(9)  | 14.269(4)  |
| β/deg                                   | 94.36(1)  | 107.58(2)   | 97.56(3)   | 103.85(2)  |
| V/Å <sup>3</sup>                        | 4908.6(8)   | 2654.3(9)   | 4615.1(4)  | 2199.1(1)  |
| Z                                       | 4   | 4   | 4  | 4  |
| T/K                                     | 293(2)  | 293(2)  | 293(2)   | 293(2)   |
| D/g cm <sup>-3</sup>                    | 2.094   | 2.026   | 1.683  | 1.742  |
| μ(Mo Kα)/mm <sup>-1</sup>               | 7.397   | 6.777   | 4.011  | 1.227  |
| reflens colld                           | 21 835  | 5062  | 4293   | 4151   |
| unique reflens                          | 7155  | 4864  | 4042   | 3851   |
| reflens with I ≥ 2σ(I)                  | 5657  | 3217  | 3312   | 3322   |
| abs corr                                | SADABS  | ψ-scans   | ψ-scans  | ψ-scans  |
| T <sub>min</sub> , T <sub>max</sub>     | 0.62–1.00   | 0.48–1.00   | 0.58–1.00  | 0.93–1.00  |
| R <sub>1</sub> <sup>a</sup>             | 0.0286  | 0.0545  | 0.0329   | 0.0225   |
| wR <sub>2</sub> (all data) <sup>b</sup> | 0.0721  | 0.1631  | 0.0818   | 0.0626   |

$$^a R_1 = \sum |F_o| - |F_c| / \sum |F_o|, \quad ^b wR_2 = \{\sum [w(F_o^2 - F_c^2)^2] / \sum [w(F_o^2)^2]\}^{1/2}.$$

heteroaromatic moiety upon interaction with metal centers. Our results with Pb<sup>II</sup>, Cd<sup>II</sup>, and Hg<sup>II</sup> show that L<sup>1</sup>–L<sup>3</sup> can be used in this respect, though their selectivity of binding needs to be improved by changing the structural and donor characteristics of the aliphatic portion of the rings. Remarkably, L<sup>3</sup> seems to be already quite selective for Pb<sup>II</sup> as the CHEQ effect recorded in the presence of this metal ion is much more pronounced, compared to that observed in the presence of Cd<sup>II</sup> or Hg<sup>II</sup>. Interestingly, the effect recorded on the fluorescence emission of L<sup>2</sup> upon addition of Cd<sup>II</sup> is markedly different from that observed on adding Pb<sup>II</sup> or Hg<sup>II</sup>, and this already represents a significant starting point in the design of specific fluorometric chemosensors on the basis of mixed-donor macrocycles containing the phenanthroline moiety.

**Acknowledgment.** We thank the “Regione Autonoma della Sardegna” and the Università degli Studi di Cagliari for financial support.

**Supporting Information Available:** Tables for mass-balance equations for the three complexation models adopted, solution of the mass-balance equations in terms of the metal ion [M] or free ligand concentrations [L], and the equations for  $F_T$ , tables giving details of the X-ray crystal structure analyses and crystallographic data in CIF format, and computer fits of fluorescence intensity/molar ratio data obtained from the complexation of L<sup>1</sup>–L<sup>3</sup> with Pb<sup>II</sup>, Cd<sup>II</sup>, and Hg<sup>II</sup>. This material is available free of charge via the Internet at <http://pubs.acs.org>.

IC020270D